Food Chemistry 271 (2019) 232–238

Contents lists available at ScienceDirect

Food Chemistry

journal homepage: www.elsevier.com/locate/foodchem

Analytical Methods

Magnetic solid phase extractions of Co(II) and Hg(II) by using magnetized *C. micaceus* from water and food samples

Sadin Özdemir[a,*], Siham Abdullah Mohamedsaid[b], Ersin Kılınç[c,*], Mustafa Soylak[d]

[a] *Food Processing Programme, Technical Science Vocational School, Mersin University, TR-33343 Yenisehir, Mersin, Turkey*
[b] *Deparment of Biology, Faculty of Science and Arts, Siirt University, 56100 Siirt, Turkey*
[c] *Health Services Vocational High School, Medical Marketing and Promotion Programme, Mardin Artuklu University, 47200 Mardin, Turkey*
[d] *Department of Chemistry, Faculty of Sciences, Erciyes University, 38039 Kayseri, Turkey*

ARTICLE INFO

Keywords:
C. micaceus
Magnetic solid phase extraction
Preconcentration
Co(II)
Hg(II)

ABSTRACT

A new bio-MSPE sorbent based on the use of *C. micaceus* and γ-Fe_2O_3 magnetic nanoparticle was prepared for the preconcentrations of Co(II) and Hg(II). Critical parameters including pH, flow rate, quantity of *C. micaceus*, quantity of γ-Fe_2O_3 magnetic nanoparticle, eluent (type, concentration and volume), sample volume, and foreign ions were examined. Surface structure and variations after interaction with Co(II) and Hg(II) of bio-MSPE sorbent were investigated by FT-IR, SEM, and EDX. The impact of bio-MSPE column reusage was also tested. The biosorption capacities were determined as 24.7 mg g^{-1} and 26.2 mg g^{-1}, respectively for Co(II) and Hg(II). Certified reference materials were utilized to find out the accuracy of the prepared bio-MSPE method. This novel bio-MSPE method was accomplished by being applied to real food and water samples. In particular, it will be possible to make use of *C. micaceus* as new alternatives, in environmental biotechnology applications.

1. Introduction

It is well known that metals are naturally available in earth's crust. An important group of periodic table metals are highly used in electronics, engineering, medicine, building materials, etc., which are characterized with features such as hardness, malleability, shiny and high thermal and electrical conductivity. Due to environmentally occurring and high usage in industry, the concentrations of metal ions should be monitored. Among metals, 23 elements with a specific gravity 5 times higher than water, are classified as heavy metals (Zawierucha, Kozlowskia, & Malinab, 2015). According to recent technical report by the International Union of Pure and Applied Chemistry (IUPAC), 'heavy metal' term has no authoritative definition but the toxicity of these related metal ions may be an alternative to their description (Duffus, 2002). The Agency for Toxic Substances and Disease Registry (ATSDR) listed the chemicals by considering their toxicity and hazardous effects. As, Pb, Hg, Cd, Be, Co, Ni, Zn, Cr, U, Th, Cu, Ba, Mn, Se, Pd, and V are metals ions that are accepted and listed as hazardous substances by ATSDR. However, some of them are also basic for the human body as parts of biochemical pathways, and/or reactions, and enzymes, as well as nutritionally. (https://www.atsdr.cdc.gov/spl/).

It is highlighted that toxic metal ions could produce reactive radicals that cause damage to DNA, lipids and proteins (Valko, Morris, & Cronin, 2005). Humans and animals are exposed to toxic metal ions because of daily diets and the environment due to anthropogenic factors. Additionally, it is worth mentioning that cancer is an inevitable result of long-term exposure to some toxic metal ions (Jaishankar, Tseten, Anbalagan, Mathew, & Beeregowda, 2014)

Co has been found in many tissues such as heart, liver, and lung because of the fact that it is an essential part of Vitamin B12. The analysis of Co in urine is accepted as biological monitoring of Co due to excretion through urine. It was reported in studies that the exposure to Co interferes DNA repair processes, the interaction of proteins with DNA, and directly damages the DNA. Oxidative stress was observed while A549 cells were exposed to Co (Valko et al., 2005). The use of Co to treat anemia ended due to its toxicity (Paustenbach, Tvermoes, Unice, Finley, & Kerger, 2013). Problems in vision and thyroid had been reported for people that were exposed to Co during the treatment of anemia. People that work in refining and mining of Co could be possible exposed to high amounts of Co. For example, breathing problems were observed among workers that breathed 0.038 ng m^{-3} of Co. Increasing in the amount of hemoglobin and erythrocyte was reported for humans and rats after the exposure to Co. The exposure to Co on skin resulted in dermatitis (US Department of Health and Human Service, 2004). The particulate form of Co and its compounds are released to the

---

* Corresponding authors.
E-mail address: sadinozdemir@mersin.edu.tr (S. Özdemir).

https://doi.org/10.1016/j.foodchem.2018.07.067
Received 18 December 2017; Received in revised form 11 June 2018; Accepted 11 July 2018

atmosphere (Co < 1–2 ng m^{-3} in unpolluted sites). It was reported that surface water and groundwater Co concentrations in pristine and populated areas are lower than 1 μg L^{-1} and 1–10 μg L^{-1} respectively. Sugar, refined and fresh cereal, green vegetables, and fish are major sources of Co intake. It was reported that 88% of Co was received from plant products in Japanese diet (WHO, Concise International Chemical Assessment Document 69).

Hg and its compounds are known to be reason for many disorders after their exposure. Mortality was observed for rats after 2 h exposure to Hg at vapor phase with a concentration of 27 mg m^{-3}. At lower concentrations, pulmonary congestion was also reported for rats. Mortality was also observed for rabbits after exposure to Hg for about 20 h. The use of Hg in dental amalgam was restricted due to its toxicity. In 1990, it was estimated that there were about 100 million of amalgam filling events in USA. Dental amalgam contains 50% of Hg, and the rest is Ag and small amounts of Cu, Sn and Zn (Soni et al., 2012). On the other hand, the management of dental amalgam waste is also a problem. It was also highlighted that amalgam fillings could be a reason of Alzheimer disease, resistance to antibiotics, autism and problems in the cardiovascular system (The International Academy of Oral Medicine and Toxicology, 2016).

Commercial resins such as Amberlite XAD-4, XAD-2010, XAD-2, XAD-16, XAD-2000, and Diaion SP-850, inorganic sorbents such as silica gel, alumina, bentonite, sepiolite, polyurethane foam and nanomaterials are reported as solid phase sorbents for SPE (Elci, Soylak, & Dogan, 1992; Soylak & Elci, 1997). However, further functionalities are required to improve the efficiency of surface through analytes.

Particle size, pore size, surface area and surface functional structure are important parameters for sorbents. The nature of analytes, as organic and inorganic, depends on the surface functionality. Nowadays multiple materials are used as SPE sorbents, called multi-mode SPE (Jenkins, Young, Mallet, & Elian 2004; Wang et al., 2015). In recent years, particles at nanometer sizes, called nanoparticles, have attained special interest due to their extraordinary properties in natural sciences, engineering and industry (Silva et al., 2011).

In addition to these Fe, Cu, Ni, Mn, and Mg oxides could also be used as core material for superparamagnetic nanomaterials (Kandasamy & Maity, 2015). Amorphous silica, mesoporous silica, polyethylene glycol, polyvinyl alcohol, polyvinyl pyrrolidine, polyacrylic acid, polystyrene, polymethyl methacrylate, polydipyrrole/dicarbazole, ethyl cellulose, chitosan, dextran, starch, liposome, albumin, erythrocytes, and gelatin have been reported as coating materials for surface modifications of super paramagnetic iron oxide nanoparticles (SPIONs) through biomedical applications (Mahmoudi, Sant, Wang, Laurent, & Sen, 2011). TiO_2, Al_2O_3, FeS, MWCNT, ZrO_2, SiO_2, MnO, and CeO_2 have also been used as nanoparticles for the preconcentration of organic and inorganic environmental pollutants before their instrumental measurements (Kaur & Gupta, 2009).

In this research *Coprinus micaceus* was used as a biosorbent. It is mostly named Mica Cap. *C. micaceus* has inky caps and leaves a black waste that looks like ink, when the gills digest themselves (deliquesce) to release spores. Their pileus is oval shaped when *C. micaceus* is young and becomes convex as it ages. These mushrooms are saprotrophic species and grow on decaying wood from April to October. It is thought to be edible but mostly tasteless. It is a very widespread mushroom and has been found in North America, northern Africa, Europe, South Africa, India, Australia, South America, Japan, and New Zealand. It can be found in both urban lawns and forests (https://en.wikipedia.org/wiki/Coprinellus_micaceus).

In the last decade, nanoparticles including carbon nanotubes, nanodiamonds, magnetic nanoparticles and organisms are used for the separation and preconcentration of metal ions prior their instrumental detections, due to their interaction between metal ions, their resistivity to acid and base and their high surface areas. In our study, fungal biomass, *C. micaceus* were immobilized on iron nanoparticles and used to investigate the magnetic solid phase extractions of Co(II) and (Hg) in food samples. In literature, there are not enough studies on magnetic solid phase extraction of heavy metals by fungal biomass and especially *C. micaceus*. From this point of view, *C. micaceus* was used in this investigation. We here indicate the usefulness of the *C. micaceus* loaded with γ-Fe_2O_3 magnetic nanoparticles to pre-concentrate the Co(II) and Hg(II) ions in food and various water samples.

2. Materials and methods

2.1. Biologic materials

C. micaceus was used as a biosorbent which was collected from Afyonkarahisar in Turkey.

2.2. Preparation of C. micaceus for loading

C. micaceus was cleaned twice with distilled water to remove contaminants after being collected and then dried at 25 °C for a week. The dried *C. micaceus* was ground in a porcelain mortar to get a fine powder. The fungal biosorbent was then kept at 80 °C in an oven for one day to kill all of the fungal cells. Finally, *C. micaceus* was inoculated to malt agar at room temperature for two days. The absence of growth of *C. micaceus* mycelia in medium indicated positive results, which means the complete death of the fungal cells.

2.3. Synthesis of magnetic ironoxide nanoparticles and loading of C. micaceus on magnetic iron oxide nanoparticles

The γ-Fe_2O_3 magnetic nanoparticles were synthesized according to Kilinc (2016) and loaded with *C. micaceus* and prepared according to Kilinc, Dundar, Ozdemir, and Okumus (2013) with some modifications.

2.4. Surface characterization of the magnetized fungal biosorbents

The surface of bio-MSPE sorbent was investigated by FT-IR and SEM-EDX to understand the micro and macro structure. Co(II) and Hg (II) were also added to the biosorbents to understand the interaction of targeted ions with functional groups on them. Co(II) and Hg(II) solutions (50 mL of 1 mg L^{-1}) at the best pH were mixed with *C. micaceus,* immobilized with γ-Fe_2O_3 magnetic nanoparticles, at 120 rpm for 2 h at 25 °C using a shaker. After 2 h, magnetic fungal biosorbents were separated from the solution using a magnet. The magnetized fungal biosorbents were then dried in an oven at 60 °C for 24 h. FT-IR analyzes were recorded with the Perkin-Elmer Spectrum 400 spectrometer. SEM and EDX analyzes were obtained with a LEO 440 SEM with an accelerating voltage of 20 kV to investigate surface characterization. The samples were covered with Au/Pd before SEM images (Ozdemir, Kilinc, Okumus, Çelik, & Soylak, 2017).

2.5. Column preparation for magnetic solid phase extraction

C. micaceus immobilized with γ-Fe_2O_3 magnetic nanoparticles (100 mg) was added to 5 mL of purified water and mixed until homogeneous in the magnetic stirrer for 120 min. The column was thoroughly washed with 1.0 M HCl and purified water, respectively before use, and then the mixture was slowly added to a 1.0 cm × 10.0 cm size of polyethylene column (Ozdemir & Kilinc, 2012).

2.6. General biosorption studies

The 30.0 mL of model solutions containing 0.5 mg L^{-1} of Co(II) and Hg(II) were prepared by diluting the stock metal solution. The pH of model solution was adjusted to the requested value. This solution was then passed through the magnetic solid-phase extraction (MSPE) column by a peristaltic pump. After passing the metal solution, distilled water (5.0 mL) was passed through the MSPE column. The retained Co

(II) and Hg(II) ions on the fungal biosorbents were then eluted with 5.0 mL of 1.0 mol L^{-1} HCl. The concentrations of Co(II) and Hg(II) ions in solution were simultaneously determined by ICP-OES.

2.7. Reusage of MSPE column

30 mL of 0.5 mgL^{-1} Co(II) and Hg(II) solutions were passed through magnetic solid phase extraction columns under the optimum conditions. The amounts of Co(II) and Hg(II) were then determined by ICP-OES after recovery with 1.0 M of 5 mL HCl. In the case of use up to 35 times, the amount of recovery was calculated. With calculations, the reusage of the column efficiency was determined.

2.8. Capacity of column

Co(II) and Hg(II) solutions (100 mL of 10 mg L^{-1}) at the best pH values were mixed with magnetized *C. micaceus*, at 120 rpm for 2 h at 25 °C using a shaker. The magnetized fungal biosorbents were then separated from the solution using a magnet. The remaining amount of metal in the supernatant liquid was measured by ICP-OES to determine biosorption capacities (Sahin & Ozturk, 2005). The metal biosorption capacities (mg of metal/g of dry cell) of magnetized fungal biosorbents were calculated according to the following equation.

$$Q = V\ (C_i{-}{-}C_f)/1000\,M$$

Q = Specific metal reception (mg of metal/g of biosorbent)
V = Volume of metal solution (mL)
C_i = Initial metal concentration in solution (mgL^{-1})
C_i = Final metal concentration in solution (mg L^{-1})
M = Amount of biosorbent (g)

2.9. Sample preparation

NWTM-15 fortified water, 1643e trace elements in water, EU-L-2 waste water and DORM2 (dog fish muscle certified reference material for trace metals) were employed as certified samples. 100 mL portions of liquid samples were subjected to MSPE procedure after pH adjustment. Founded values were compared with certified values to evaluate the accuracy of the method. Tap water was sampled from Siirt and Diyarbakır after flushing for 5.0 min. Mineral water was bought from local markets in 1.0 L plastic bottles. Dicle, Botan, and Kezer Rivers waters were sampled in a 5.0 L PTFE bottle and acidified with 3 drops of concentrated nitric acid. After pH adjustment, the method was applied to water samples. Potato, cabbage, ketchup, green pepper, meat, tuna fish, chicken, and milk were bought from local markets, too. The samples were digested by a method given in our previous study (Ozdemir et al., 2017).

3. Results and discussion

3.1. FT-IR and SEM results for surface investigations

FT-IR analyzes of *C. micaceus* immobilized γ-Fe_2O_3 magnetic nanoparticles, *C. micaceus* immobilized γ-Fe_2O_3 magnetic nanoparticles with Co(II) and Hg(II) are represented in Fig. 1. The surface functionalities of synthesized magnetic nanoparticles were determined by considering the spectroscopic results from FT-IR studies. The peaks at 500, 1500, and 3200–3300 cm^{-1} were characteristic peaks for Fe—O vibrations of γ-Fe_2O_3, attributed to carboxyl and groups of fungal biosorbents and the presence of surface hydroxyls of γ-Fe_2O_3, respectively (Fig. 1a). The peaks on 811, 1259, 1394, and 3676 cm^{-1} in Fig. 1b were evaluated as biosorptions after Co(II) immobilization. The double sharper peaks observed at 1300 and 2900 cm^{-1} and shifting on other peaks at about 10 cm^{-1} were attributed to biosorption. The peaks on 1205 and 1148 cm^{-1} in Fig. 1c were evaluated as biosorption after Hg(II) immobilization. Approximately 10 cm^{-1} shifting on peaks was also attributed to complexation. SEM-EDX images of *C. micaceus* immobilized with γ-Fe_2O_3 magnetic nanoparticles, *C. micaceus* immobilized γ-Fe_2O_3 magnetic nanoparticle with Co(II) and Hg(II) are presented in Fig. 2. As shown, homogenous adsorption was observed for Co(II) and Hg(II). This facilitates to understand the reproducibility of the *C. micaceus* immobilized γ-Fe_2O_3 magnetic nanoparticles for preconcentration of targeted ions.

3.2. The effect of pH on the recoveries of Co(II) and Hg(II)

In solid phase extraction studies, pH is one of the most important parameters to be studied for the recovery of metal ions. The binding of metal ions depends on the ionic interaction between the functional groups of the biomass and the metal ions. The effect of pH on the recovery of Co(II) and Hg(II) using magnetic solid phase extraction columns is shown in Fig. 3. The percentage of biosorption was determined to reduce in MSPE column used at low pH degree. The optimal pH for Co(II) and Hg(II) was determined as 4.0–5.0. At low acidic pH degree (greater than4.0), metal biosorption is reduced due to competition between H^+ ions and metal ions for binding sites with metal-related biosorbent surface (Green-Ruiz, Tirado, & Gil, 2008). At high solution pH, metal ions bind to increasing OH^- groups in the environment and cause precipitation. Thus, it may be difficult to process biosorption yields (Vijayaraghavan & Yun, 2008). pH 5.0 was applied for magnetic solid phase extraction of Co(II) and Hg(II) in further studies.

3.3. Effect of flow rate

It is well known that process efficiency and time are very important in biotechnological studies. For these reasons, the flow rate is one of the important parameters to be studied in solid phase extraction studies. The impact of flow rate on the recoveries of Co(II) and Hg(II) using bio-magnetic solid phase extraction column is demonstrated on Supplementary Material 1. The flow rate did not change significantly up to 3 mL min^{-1} for the recoveries of Co(II) and Hg(II). The recovery percentages of Co(II) and Hg(II) were found as 82.4%, 70.9%, and 60.7% and 84.1%, 74.3%, and 63.9% at 4 mL min^{-1}, 5 mL min^{-1}, and 6 mL min^{-1}, respectively. As seen in Supplementary Material 1, the highest flow rates were determined as 3 mL min^{-1} for recovery of tested metal ions. As the flow rate increases, there is not enough binding time between the metal ions with metal-binding functional groups on the surface of biosorbents, resulting in yield reduction (Anthemidis, Zachariadis, & Stratis, 2001). In following experiments, 3 mL min^{-1} was used as flow rate.

3.4. Influence of quantities of C. micaceus and Fe_2O_3 magnetic nanoparticle

The influence of various quantities *C. micaceus* on the recoveries of Co(II) and Hg(II) is shown in Supplementary Material 2a. The quantities of *C. micaceus* varied from 50 to 300 mg. According to the obtained results, it was determined that Co(II) and Hg(II) recovery increased up to certain quantities of *C. micaceus*. The recovery percentages of Co(II) and Hg(II) were found as 80.1% and 96.2% and 80.7% and 96.4% at 50 and 100 mg of *C. micaceus*, respectively. The recovery of Co(II) and Hg (II) were also found as 100% at 150, 200, 250, and 300 mg of *C. micaceus*. It is indicated that as the quantity of biomass rises, the quantity of biosorbed metal ions also rises. This is due to an increase in the number of metal binding sites, depending on the amount of biomass being increased (Han et al., 2006). So, 100 mg of biomass was used for the following experiments. The amounts between 50 and 300 mg iron oxide nanoparticles were used to determine the most suitable support matrix for Co(II) and Hg(II) recovery. The influence of MSPE columns using different γ-Fe_2O_3 magnetic nanoparticle quantities on the recovery of Co(II) and Hg(II) is shown in Supplementary Material 2b. When the quantity of support matrix increased from 50 mg to 100 mg,

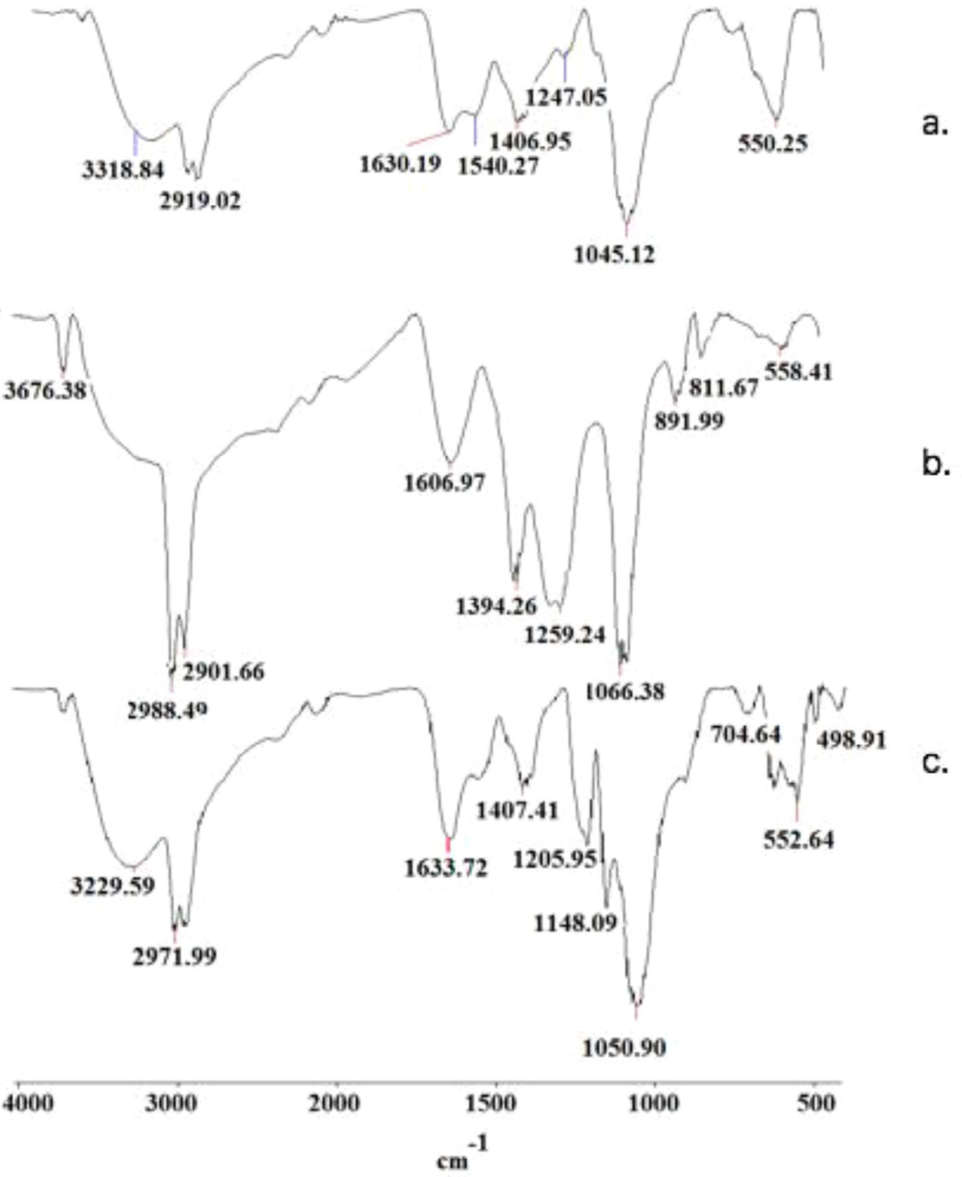

Fig. 1. FT-IR spectral comparison of a. *C. micaceus* immobilized γ-Fe_2O_3 magnetic nanoparticle b. *C. micaceus* immobilized γ-Fe_2O_3 magnetic nanoparticle with Co(II), c. *C. micaceus* immobilized γ-Fe_2O_3 magnetic nanoparticle with Hg(II).

the percentages of Co(II) and Hg(II) increased from 89.4% to 98.5% and from 90.4% to 99.1%, respectively for the bio- MSPE column. Experimental results showed that the recovery of Co(II) and Hg(II) increased up to 150 mg of γ-Fe_2O_3 magnetic nanoparticles and there was not any change in the recovery of the tested metal ions. As a result, the quantity of 100 mg iron oxide nanoparticles was utilized as support matrix in the following investigations.

3.5. Eluent type, volume and concentration of eluent

The eluent type, volume and concentration can affect the recovery efficiency and the structure of functional groups on the surface of the biosorbent. From that point of view, it is very important that the eluent concentration and volume should be low (Ozdemir, Okumus, Dundar, & Kilinc, 2013). HCI and HNO_3 were used as elution solutions. The effects of HCI and HNO_3 at different volumes and concentrations were investigated to recover two different metal ions from the magnetically charged biosorbent surface. The results are demonstrated in Supplementary Material 3. It was found that the best elution solution was conducted with 5.0 mL 1.0 mol L^{-1} HCl.

3.6. Effect of sample volume

Real samples such as river water, drinking water and ore specimens contain trace amounts of metal ions. Therefore, it is very important to know the sample volume for the determination the trace amounts of metal ions in natural samples (Ozdemir & Kilinc, 2012). In this study, it was found that as sample solution volume increased up to 400 and 500 mL, biosorption yields of Co(II) and Hg(II) did not change significantly and after this point a decrease occurred in biosorption yields. This decrease indicates that as the metal concentration is rather low in high sample volumes, the interaction of tested metal ions with magnetized fungal cells also decreases while passing through the column. Considering 400 and 500 mL as the sample volume and 5.0 mL as the eluent volume, an enrichment factor of 80 and 100 was achieved for Co and Hg(II), respectively. (Supplementary Material 4).

3.7. Foreign ions

Natural samples do not contain only tested metal ions but also foreign ions. Particularly those ions, which are present in the natural

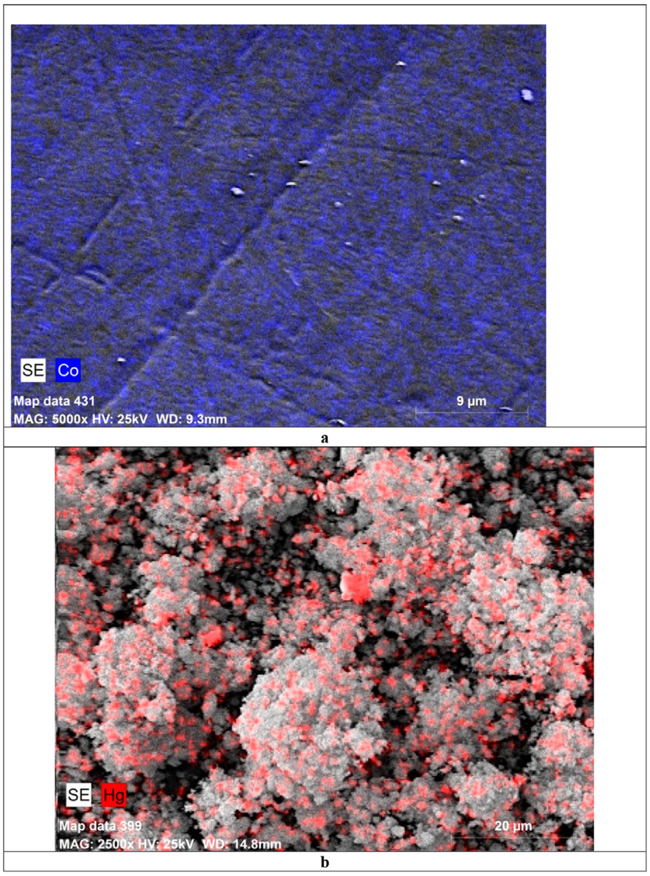

Fig. 2. SEM-EDX images of a. *C. micaceus* immobilized γ-Fe_2O_3 magnetic nanoparticle with Co(II), b. *C. micaceus* immobilized γ-Fe_2O_3 magnetic nanoparticle with Hg(II).

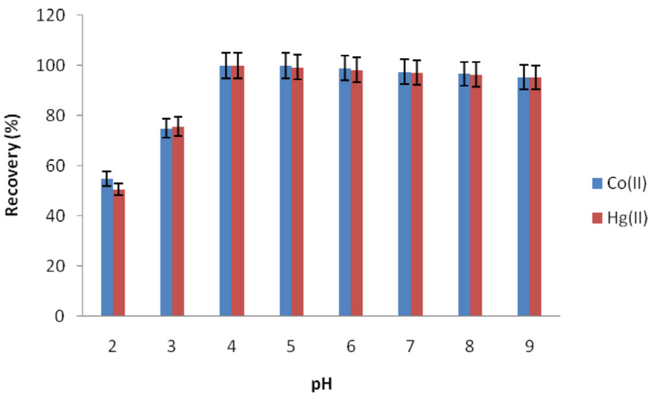

Fig. 3. Effect of pH for recoveries of Co(II) and Hg(II) (30 mL of 0.5 mg L^{-1} Co (II) and Hg(II), elution with 1.0 M of 5 mL HCl).

samples and cause the matrix effect, affect the efficiency of the metal recovery. Various concentration of foreign ions such as Na(I), K(I), Ca (II), Mg(II), Fe(II), Al(III), Cr(III), Fe(III), Sn(II), As(III), Pb(II), Ni(II), Cu(II), Cd(II), and Zn(II) were added into Co(II) and Hg(II) solutions and the magnetic solid phase extraction method was performed for the determination of the effects of foreign ions for recoveries of Co(II) and Hg(II). Results indicated that all foreign ions did not significantly affect the recovery values as represented in Supplementary Material 5.

3.8. Bio-MSPE column reusage and capacity

It is biotechnologically crucial that rate of solid phase extraction columns reusability should be high. As seen in Supplementary Material 6, the recovery percentages were 100% after 25 reusages of bio-MSPE column for both metal ions. Following 35 uses of bio-MSPE column in this investigation, quantitative recovery yield of Co(II) and Hg(II) was also found to be more than 95%. This is very important for the application of the MSPE process in biotechnological studies. Also, this research study investigated to what extent a column substance at a certain amount could hold Co(II) and Hg(II), that is to say, how much the biosorption capacity was. Thus, under optimum conditions, 20 mg immobilized biosorbents were mixed for 120 min at 120 rpm with 100 mL 10 mg L^{-1} Co(II) and Hg(II) solution. Then, magnetic-loaded biosorbents were removed from suspension through nickel magnet. Biosorption capacities were determined by quantifying residual Co(II) and Hg (II) in the aqueous solution. Biosorption capacities were found 24.7 mg g^{-1} and 26.2 mg g^{-1}, respectively for Co(II) and Hg(II) using *C. micaceus*-MSPE column.

3.9. Analytical figures of merit

Analytical figures of merit of the method based on the use of *C. micaceus* immobilized γ-Fe_2O_3 magnetic nanoparticle for preconcentration of Co(II) and Hg(II) are listed in Supplementary Material 7 in view of LOD, LOQ, RSD, linear range, correlation coefficient, and preconcentration factor. It could be discussed that the developed method presents low LOD, high preconcentration factor and wide linear range in comparison with literature (Table 1). Additionally, the use of synthetic ligands was eliminated. The accuracy of the developed method was controlled by applying to NWTM-15 fortified water, 1643e trace elements in water, EU-L-2 waste water and DORM2 (dog fish muscle certified reference material for trace metals). Founded values after the MSPE procedure was applied were compared with certified ones. The results agreed with certified values (Table 2). So, the developed method can be applied to real samples. The applicability of the recommended method was tested on real samples. For this purpose, concentrations of Co(II) and Hg(II) in water and food samples were determined by ICP-OES after the developed method was applied (Table 3).

4. Conclusions

C. micaceus was immobilized to magnetica ironoxide nanoparticles. This novel bio-magnetized solid phase extractor was used for preconcentrations of Co(II) and Hg(II) before their determinations by ICP-OES. The surface structure and interactions with Co(II) and Hg(II) of new bioMSPE sorbents was investigated by FT-IR, SEM, and EDX. Several parameters were tested to determine the best operation conditions. Then, the accuracy of the bio-MSPE method was studied by using certified reference samples. The practicality of the novel bio-MSPE method was applied to real samples. As a result, immobilized *C. micaceus* used in this study by magnetic solid phase extraction, shows potential application in the preconcentration of Co(II) and Hg(II) in natural real samples.

Acknowledgement

This academic work was linguistically supported by the Mersin Technology Transfer Office Academic Writing Center of Mersin University, Turkey.

Appendix A. Supplementary data

Supplementary data associated with this article can be found, in the online version, at https://doi.org/10.1016/j.foodchem.2018.07.067.

Table 1
Comparison of analytical characteristics of the preconcentration methods for Co(II) and Hg(II).

Method	Instrument	LOD, ng mL^{-1}		PF[1]		Linear range, ng mL^{-1}		Ref.
		Co(II)	Hg(II)	Co(II)	Hg(II)	Co(II)	Hg(II)	
SPE on Amberlite XAD-2 resin anchored with pyrocatechol	FAAS	0.95	–	24	–	–	–	Lemos et al. (2006)
Vortex assisted magnetic SPE on silica coated magnetic multiwalled carbon nanotubes impregnated with 1-(2-pyridylazo)-2-naphthol	FAAS	0.55	–	15	–	–	–	Khan et al. (2016)
Ligand-less *in situ* surfactant-based solid phase extraction	FAAS	1.0	–	37.6	–	3–300	–	Mohammadi, Afzali, Fallahi, Mehrabi, and Moslemi (2015)
Magnetic SPEon magnetic core–shell nanoparticles modified with thiourea-derived chelating agents	Direct mercury analyzer	–	0.017	–	100	–	–	Yang, Sheng, Kaiju, Yangzhong, and Zhangjun (2015)
Preconcentration on dithizone/sodium dodecyl sulfate-immobilized on alumina-coated magnetite nanoparticles	Cold vaporAAS	–	0.058	–	250	–	0.2–80	Karimi, Hatefi-Mehrjardi, and Kabir (2014)
Preconcentration on an ion imprinted polymer coated maghemite nanoparticles	FAAS	–	4.1	–	100	–	20–1000	Tayyebeh, Borhan, Mazaher, and Abbas (2015)
SPE on *C. micaceus* immobilized γ-Fe$_2$O$_3$ magnetic nanoparticle	ICP-OES	0.017	0.04	80	80	0.25–12.5	0.25–12.5	**This study**

Table 2
Accuracy of the method for *C. micaceus* immobilized Fe$_2$O$_3$ magnetic nanoparticle.

Sample	Co(II), ng mL^{-1}		Hg(II), ng mL^{-1}	
	Certified	Founded	Certified	Founded
NWTM-15	15.1	14.9 ± 0.9	–	–
1643e	27.06 ± 0.32	26.84 ± 1.1	–	–
EU-L-2	81	80 ± 4	–	–
DORM-2[1]	0.182 ± 0.031	0.178 ± 0.022	4.64 ± 0.26	4.61 ± 0.35

[1] ng g^{-1}.

Table 3
Applicability of the developed methods to real samples.

Sample	*C. micaceus* immobilized γ-Fe$_2$O$_3$ magnetic nanoparticle	
	Co(II), ng mL^{-1}	Hg(II), ng mL^{-1}
Tap water, Siirt	3.0 ± 0.020	< LOD
Tap water, Diyarbakır	3.2 ± 0.034	< LOD
Mineral water	5.4 ± 0.039	< LOD
Van Lake	4.7 ± 0.053	< LOD
Dicle River	4.1 ± 0.051	< LOD
Botan River	3.8 ± 0.043	< LOD
Kezer River	4.6 ± 0.049	< LOD
Potato	35.4 ± 4.5	< LOD
Cabbage	24.4 ± 2.2	< LOD
Ketchup	26.4 ± 1.1	< LOD
Green pepper	18.6 ± 1.3	< LOD
Meat	34.5 ± 2.9	< LOD
Tuna fish	10.1 ± 0.8	1.1 ± 0.08
Chicken	15.0 ± 1.3	< LOD
Milk	9.8 ± 0.6	< LOD

References

Anthemidis, A. N., Zachariadis, G. A., & Stratis, J. A. (2001). On-line solid phase extraction system using PTFE packed column for the flame atomic absorption spectrometric determination of copper in water samples. *Talanta, 54*, 935–942.

Duffus, J. H. (2002). Heavy metals-a meaningless term? IUPAC technical report. *Pure and Applied Chemistry, 74*, 793–807.

Elci, L., Soylak, M., & Dogan, M. (1992). Preconcentration of trace metals in river waters by the application of chelate adsorption on Amberlite XAD-4. *Fresenius Journal of Analytical Chemistry, 342*, 175–178.

Green-Ruiz, C., Tirado, V. R., & Gil, B. G. (2008). Cadmium and zinc removal from aqueous solutions by *Bacillus jeotgali*: pH, salinity and temperature effects. *Bioresource Technology, 99*, 3864–3870.

Han, R., Li, H., Li, Y., Zhang, J., Xiao, H., & Shi, J. (2006). Biosorption of copper and lead ions by waste beer yeast. *Journal of Hazardous Materials, 137*, 1569–1576.

https://en.wikipedia.org/wiki/Coprinellus_micaceus (accessed on 09.02.2017).

https://www.atsdr.cdc.gov/spl/ (accessed on 09.02.2017).

Jaishankar, M., Tseten, T., Anbalagan, N., Mathew, B. B., & Beeregowda, K. N. (2014). Toxicity, mechanism, and health effects of some heavy metals. *Interdisciplinaary Toxicology, 7*, 60–72.

Jenkins, K. M., Young, M. S., Mallet, C. R., & Elian, A. A. (2004). Mixed-mode solid-phase extraction procedures for the determination of MDMA and metabolites in urine using LC-MS, LC-UV, or GC-NPD. *Journal of Analytical Toxicology, 28*, 50–58.

Kandasamy, G., & Maity, D. (2015). Recent advances in super paramagnetic ironoxide nanoparticles (SPIONs) for *in vitro* and *in vivo* cancer nanotheranostics. *International Journal of Pharmaceutics, 496*, 191–218.

Karimi, M. A., Hatefi-Mehrjardi, A., & Kabir, A. A. (2014). Application of modified magnetite nanoparticles as a new sorbent for separation/preconcentration of mercury (II) trace amounts and its determination by cold vapor atomic absorption spectrometry. *Croatica Chemica Acta, 87*, 129–136.

Kaur, A., & Gupta, U. (2009). A review on applications of nanoparticles for the preconcentration of environmental pollutants. *Journal of Materials Chemistry, 19*, 8279–8289.

Khan, M., Yilmaz, E., Sevinc, B., Sahmetlioglu, E., Shah, J., Jan, M. R., & Soylak, M. (2016). Preparation and characterization of magnetic allylamine modified graphene oxide-poly(vinyl acetate-co-divinylbenzene) nanocomposite for vortex assisted magnetic solid phase extraction of some metal ions. *Talanta, 146*, 130–137.

Kilinc, E. (2016). γ-Fe$_2$O$_3$ magnetic nanoparticle functionalized with carboxylated multiwalled carbon nanotube: Synthesis, characterization, analytical and biomedical application. *Journal of Magnetism and Magnetic Materials, 401*, 949–955.

Kilinc, E., Dundar, A., Ozdemir, S., & Okumus, V. (2013). Solid phase extraction based on the use of *Agaricus arvensis* as a fungal biomass for the preconcentrations of Pb and Al prior to their determination in vegetables by ICP-OES. *Atomic Spectroscopy, 34*, 78–88.

Lemos, V. A., Silva, D. G., Carvalho, A. L., Santana, D. A., Novaes, G. S., & Passos, A. S. (2006). Synthesis of amberlite XAD-2-PC resin for preconcentration and determination of trace elements in food samples by flame atomic absorption spectrometry. *Microchemical Journal, 84*, 14–21.

Mahmoudi, M., Sant, S., Wang, B., Laurent, S., & Sen, T. (2011). Superparamagnetic iron oxide nanoparticles (SPIONs): Development, surface modification and applications in chemotherapy. *Advanced Drug Delivery Reviews, 63*, 24–46.

Mohammadi, S. Z., Afzali, D., Fallahi, Z., Mehrabi, A., & Moslemi, S. (2015). Ligand-less *in situ* surfactant-based solid phase extraction for preconcentration of cobalt, nickel and zinc from water samples prior to their FAAS determination. *Journal of Brazilian Chemistry Society, 26*, 51–56.

Ozdemir, S., & Kilinc, E. (2012). *Geobacillus thermoleovorans* immobilized on Amberlite XAD-4 resin as a sorbent for solid phase extraction of uranium(VI) prior to its spectrophotometric determination. *Microchimica Acta, 178*, 389–397.

Ozdemir, S., Kilinc, E., Okumus, V., Çelik, K. S., & Soylak, M. (2017). Simultaneous preconcentrations of Co^{2+}, Cr^{6+}, Hg^{2+} and Pb^{2+} ions by *Bacillus altitudinis* immobilized nanodiamond prior to their determinations in food samples by ICP-OES. *Food Chemistry, 215*, 447–453.

Ozdemir, S., Okumus, V., Dundar, A., & Kilinc, E. (2013). Preconcentration of metal ions using microbacteria. *Microchimica Acta, 180*, 719–739.

Paustenbach, D. J., Tvermoes, B. E., Unice, K. M., Finley, B. L., & Kerger, B. D. (2013). A review of the health hazards posed by cobalt. *Critical Reviews in Toxicology, 43*, 316–362.

Sahin, Y., & Ozturk, A. (2005). Biosorption of chromium(VI) ions from aqueous solution by the bacterium *Bacillus thuringiensis*. *Process Biochemistry, 40*, 1895–1901.

Silva, B. F., Perez, S., Gardinalli, P., Singhal, R. K., Mozeto, A. A., & Barcelo, D. (2011). Analytical chemistry of metallic nanoparticles in natural environments. *Trends in Analytical Chemistry, 30*, 528–540.

Soni, R., Bhatnagar, A., Vivek, R., Singh, R., Chaturvedi, T. P., & Singh, A. (2012). A systematic review on mercury toxicity from dental amalgam fillings and its management strategies. *Journal of Scientific Research, 56*, 81–92.

Soylak, M., & Elci, L. (1997). Preconcentration and separation of trace metal ions from sea water samples by sorption on Amberlite XAD-16 after complexation with sodium diethyldithiocarbamate. *International Journal of Environmental Analytical Chemistry, 66*, 51–59.

Tayyebeh, M., Borhan, Z., Mazaher, A., & Abbas, A. (2015). Selective extraction and sensitive determination of mercury (II) ions by flame atomic absorption spectrometry after preconcentration on an ion-imprinted polymer-coated maghemite nanoparticles. *Journal of Iran Chemical Society, 12*, 1235–1243.

The International Academy of Oral Medicine and Toxicology, Report. (2016). A comprehensive review of the toxic effects of mercury in dental amalgam fillings on the environment and human health.

US Department of Health and Human Service, Public Health Service, Agency for Toxic Substances and Disease Registry. (2004). Toxicological profile for cobalt.

Valko, M., Morris, H., & Cronin, M. T. D. (2005). Metals, toxicity and oxidative stress. *Current Medicinal Chemistry, 12*, 1161–1208.

Vijayaraghavan, K., & Yun, Y. S. (2008). Bacterial biosorbents and biosorption. *Biotechnology Advance, 26*, 266–291.

Wang, W., Qin, S., Li, L., Chen, X., Wang, Q., & Wei, J. (2015). An optimized high throughput clean-up method using mixed-mode SPE plate for the analysis of free arachidonic acid in plasma by LC-MS/MS. *International Journal of Analytical Chemistry, 2015*, 374819–374825.

WHO, Concise International Chemical Assessment Document 69, Cobalt and inorganic cobalt compounds.

Yang, C., Sheng, L., Kaiju, W., Yangzhong, L., & Zhangjun, H. (2015). Magnetic solid-phase extraction of trace-level mercury(II) ions using magnetic core-shell nanoparticles modified with thiourea-derived chelating agents. *Microchimica Acta, 182*, 1337–1344.

Zawierucha, I., Kozlowskia, C., & Malinab, G. (2015). Immobilized materials for removal of toxic metal ions from surface/groundwaters and aqueous waste streams. *Environmental Sciences: Processes Impacts, 18*, 429–444.